

Article

High-Temperature Performance Evaluation of Asphalt Mixtures by Adding Short-Chopped Basalt Fiber

Xueyang Jiu ¹, Yu Wang ¹, Zhengguang Wu ^{1,2,*}, Peng Xiao ^{1,2} and Aihong Kang ^{1,2}¹ College of Civil Science and Engineering, Yangzhou University, Yangzhou 225127, China² Research Center for Basalt Fiber Composite Construction Materials, Yangzhou 225127, China

* Correspondence: zgwu@yzu.edu.cn; Tel.: +86-13852736032

Abstract: Adding basalt fiber (BF) can effectively enhance the performance of asphalt mixtures and improve the service quality of asphalt pavement. However, the effect of BF on the high-temperature performance of different types of asphalt mixtures and systematic high-temperature performance test analysis are still not well known. To address this issue, three typical types of asphalt mixtures of AC-13, SMA-13, and SUP-13 were selected. Wheel tracking test, uniaxial penetration test, dynamic modulus test, and dynamic creep test were conducted. In addition, relevant parameters of dynamic stability, penetration strength, dynamic modulus index, and flow number were analyzed. The results showed that adding BF into the asphalt mixture could improve the dynamic stability, penetration strength, dynamic modulus index, and flow number significantly, indicating that adding basalt fiber is an effective solution to the rutting deformation damage of asphalt pavement. Moreover, the parameter of dynamic stability presented an approximate polynomial correlation with penetration strength, dynamic modulus index, and flow number, respectively. These findings provide a certain theoretical reference for evaluating the high-temperature performance of BF-modified asphalt mixtures.

Keywords: basalt fiber; asphalt mixtures; high-temperature performance; correlation analysis



Citation: Jiu, X.; Wang, Y.; Wu, Z.; Xiao, P.; Kang, A. High-Temperature Performance Evaluation of Asphalt Mixtures by Adding Short-Chopped Basalt Fiber. *Buildings* **2023**, *13*, 370. <https://doi.org/10.3390/buildings13020370>

Academic Editors: Romain Balieu, Liang He, Augusto Cannone Falchetto and Jiqing Zhu

Received: 8 December 2022

Revised: 7 January 2023

Accepted: 27 January 2023

Published: 29 January 2023



Copyright: © 2023 by the authors. Licensee MDPI, Basel, Switzerland. This article is an open access article distributed under the terms and conditions of the Creative Commons Attribution (CC BY) license (<https://creativecommons.org/licenses/by/4.0/>).

1. Introduction

Asphalt pavement has already become the main high-grade pavement form in China because of its unique advantages. After decades of development, the performance of asphalt pavement has made great progress. However, with the rapid development of the national economy, the passenger and cargo transport volume of high-grade highways increased rapidly, which led to various diseases of asphalt pavement. Among them, high-temperature deformation damages, such as rutting and upheaval, will appear on asphalt pavements and deteriorate rapidly under high temperatures and overload vehicle conditions [1–4]. Meanwhile, once the maintenance is not in time, deformation will accumulate, causing damage to the pavement structure and resulting in a decrease in asphalt pavement performance and service life. Enhancing the high-temperature deformation resistance of mixtures has become one of the hot issues in the asphalt industry [5–8].

The application of fiber into asphalt mixture is one of the most common solutions for researchers to improve the high-temperature performance of asphalt mixture by changing its material composition [9–11]. Fiber-modified asphalt mixture is a kind of physical synthesis composite material. At present, the main fiber types applied in asphalt mixture to improve pavement performance include lignin fiber, mineral fiber, polymer fiber, glass fiber, and so on. Among these, as a new environmentally friendly mineral fiber, basalt fiber has gained more attention for the improvement of asphalt pavement performance due to its unique advantages: better strength, chemical stability, wide working temperature range, etc. It has been approved that adding basalt fiber can strengthen the pavement property of asphalt mixtures [12–16], especially the high-temperature deformation resistance and fatigue resistance [17–19]. Zhang et al. [20,21] employed a wheel tracking test and dynamic

modulus test to measure the high-temperature rutting resistance of fiber-modified asphalt mixtures. The results show that at a high temperature, adding basalt fiber into an asphalt mixture can evidently improve its stiffness. Guo et al. [22–27] studied the impact of basalt fiber on the high-temperature performance of asphalt mixtures using the Marshall stability test and wheel tracking test. The results present that adding basalt fiber can improve several high-temperature indexes of asphalt mixtures effectively.

Li et al. [28] studied the high-temperature deformation resistance of SBS-modified asphalt mixtures and pointed out that the asphalt mixtures possess better deformation resistance when the basalt fiber content is 0.25%, compared with the neat mixtures without basalt fiber. Cheng et al. [29] employed the uniaxial compression creep test and the rutting test to assess the high-temperature deformation resistance to permanent deformation of the diatomite and basalt fiber-modified asphalt mixture. Test results indicate that adding basalt fiber can reinforce the rutting resistance and slow down the creep rate. Wu et al. [30] discussed the impacts of basalt fiber on the high-temperature rutting resistance of asphalt mixtures with reclaimed asphalt pavement (RAP) contents of 0%, 30%, 40%, and 50%, based on wheel tracking tests. In addition, Zhang et al. [31] found that adding basalt fiber into asphalt mixtures can increase the dynamic stability and reduce the rutting depth of open-graded friction course (OGFC) mixtures significantly by Hamburg wheel tracking test and proposed the optimal basalt fiber dosage of 0.15%.

It can be observed that the above-mentioned literature mainly focuses on the improvement of basalt fiber on the high-temperature rutting resistance of asphalt mixtures by a single parameter, such as dynamic stability at 60 °C from wheel tracking test, dynamic modulus at high temperature from dynamic modulus test, or penetration strength from a uniaxial penetration test, etc. However, there is still a lack of comprehensive analysis of different parameters and an understanding of the relationship between pavement performance and mechanical properties.

In this paper, four different types of test methods, including wheel tracking test, uniaxial penetration test, dynamic modulus test as well as dynamic creep test, were adopted to investigate and evaluate the high-temperature performance of basalt fiber modified asphalt mixtures. Three widely used types of asphalt mixtures containing dense graded gradations AC-13, Superpave-13 (SUP-13 for short), and stone matrix SMA-13 were selected. Typical parameters from the four tests were analyzed, and the correlations were established. Then the high-temperature performance index obtained by a simple experimental method can be used to predict other high-temperature performance test indexes. It is expected that the findings can provide a reference for the evaluation of the high-temperature performance of the basalt fiber-modified asphalt mixtures.

2. Raw Materials and Test Methods

2.1. Raw Materials

2.1.1. Short-Chopped Basalt Fiber

In this paper, short-chopped basalt fiber (BF) with a length of 6 mm produced by Jiangsu Tianlong Basalt Fiber Co., Ltd., Yizheng, China, was used, as shown in Figure 1. Flocculent lignin fiber (LF), produced by JRS company, Germany, was also selected as a fiber stabilizer for neat sample of SMA-13 graded asphalt mixture for comparison, as shown in Figure 2. The properties of BF and LF are listed in Tables 1 and 2.

Table 1. The properties of BF.

Index	Elastic Modulus/Gpa	Moisture Content/%	Fracture Strength/Mpa	Combustible Content/%	Elongation at Break/%
Value	90–110	0.1	2500–5000	0.55	2.69
Requirements in T/CHTS 10016	≥80	≤0.2	≥2000	-	≥2.1



Figure 1. Basalt fiber.



Figure 2. Lignin fiber.

Table 2. The properties of LF.

Index	Ash Content/%	PH Value	Oil Absorption Rate/Times
Value	19.3	7.7	6.2
Requirements in JT/T 533-2020	13–23	6.5–8.5	5–9

2.1.2. Asphalt

The styrene butadiene styrene (SBS)-modified asphalt, provided by Tiannuo Road Materials Technology Co., Ltd., Zhenjiang, China, was selected in this research. The physical properties are summarized in Table 3.

Table 3. Physical properties of SBS-modified asphalt.

Properties	Penetration (25 °C)/0.1 mm	Ductility (5 °C, 5 cm/min)/cm	Softening Point /°C	Penetration Index (PI)	Viscosity (135 °C)/Pa·s
SBS modified asphalt	67	48	78	0.3	1.8

2.1.3. Aggregates and Mineral Powder

Basalt aggregates were used for asphalt mixtures of SMA-13 gradation, while limestone aggregates were selected for AC-13 and SUP-13. The apparent relative densities of the coarse and fine aggregates of basalt aggregates are 2.929 g/cm^3 and 2.840 g/cm^3 . In addition, the apparent relative densities of the coarse and fine aggregates of limestone aggregates are 2.750 g/cm^3 and 2.700 g/cm^3 .

2.2. Gradation Design

2.2.1. Gradation Curve

Three typical mixtures, AC-13, SMA-13, and SUP-13, were adopted. The gradation curves are illustrated in Figure 3, respectively. The AC-13 and SMA-13 gradation design processes were conducted following the procedures listed in the JTG F40-2004 [32], while SUP-13 gradation design process was in accordance with the Superpave design method.

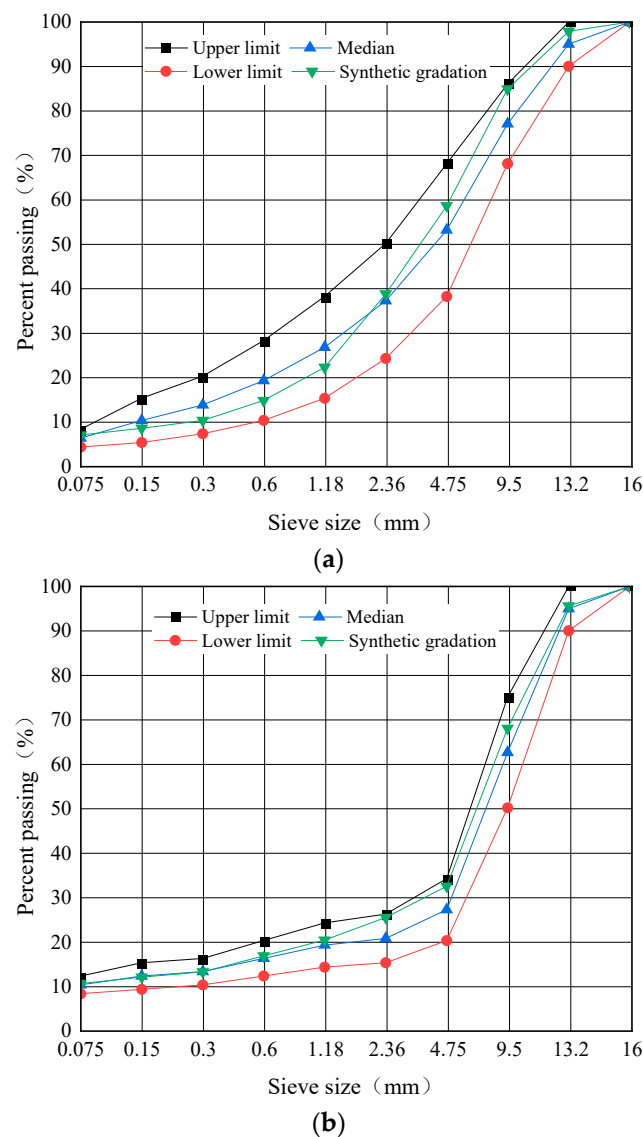


Figure 3. Cont.

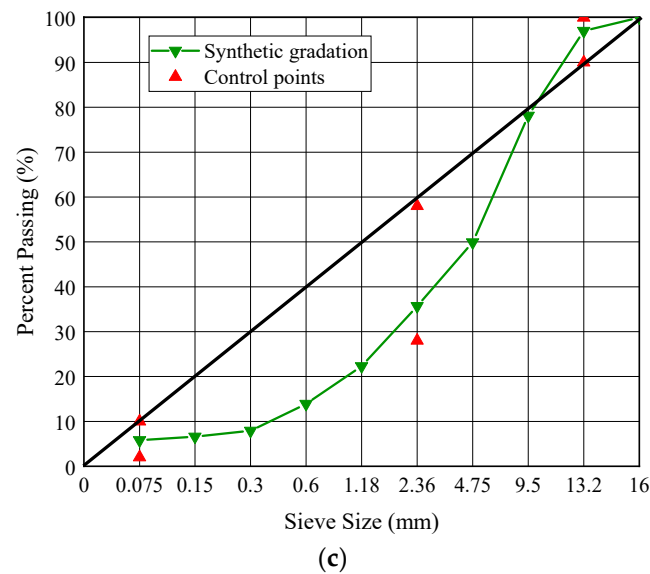


Figure 3. Gradation curves of different types of asphalt mixtures: (a) Gradation curve of AC-13; (b) Gradation curve of SMA-13; (c) Gradation curve of SUP-13.

2.2.2. Volumetric Properties of Asphalt Mixtures

The types and dosages of fiber for different asphalt mixtures are summarized in Table 4. Standard Marshall specimens were carried out by the Marshall design method, according to Chinese standard JTG E20 [33]. For each set, at least four specimens should be prepared. Every standard Marshall specimen would be compacted 75 times on both sides. The volumetric properties results of all the different types of asphalt mixtures with the corresponding optimum asphalt content (OAC) are shown in Table 5.

Table 4. Fiber usage of asphalt mixtures.

Gradation Type	Asphalt Type	Fiber Type	Fiber Dosage/%
AC-13		/	/
		BF	0.3
SMA-13	SBS modified asphalt	LF	0.3
		BF	0.3
SUP-13		/	/
		BF	0.3

Note: Fiber dosage refers to the percentage of the fiber mass to the total mixture mass

Table 5. The results of Marshall test for different asphalt mixtures.

Mixture Type	Optimum Asphalt Content/%	Marshall Stability/kN	Flow Value/mm	Air Voids/%	Voids Filled with Asphalt/%	Voids in Mineral Aggregate/%
AC-13	5.1	10.7	3.9	4.0	71.3	13.8
AC-13C+BF	5.3	10.4	3.7	4.3	70.7	14.5
SMA-13	6.1	12.0	2.4	4.3	76.0	18.0
SMA-13+BF	6.0	12.8	2.2	4.1	76.9	17.8
SUP-13	4.7	10.9	3.9	4.0	71.6	14.2
SUP-13+BF	4.8	10.9	3.8	4.2	71.6	14.7

2.3. Test Methods

2.3.1. Wheel Tracking Test

In accordance with JTG E20-T0719 [33], the wheel tracking test was conducted under the wheel pressure of 0.7 MPa. Considering the high ambient temperature in summer, the in-situ pavement temperature can be higher than 60 °C. Therefore, both 60 °C and 70 °C were selected as the test temperatures. Dynamic stability (DS), calculated by Equation (1),

was employed to evaluate the high-temperature rutting resistance of asphalt mixtures. In general, higher DS values are expected to obtain superior rutting resistance.

$$DS = \frac{(t_2 - t_1) \times N}{d_2 - d_1} \times C_1 \times C_2 \quad (1)$$

where N is the running speed of the wheel, usually 42 times/min; d_1 and d_2 are the deformations of the asphalt mixtures at the running time t_1 (45 min), t_2 (60 min), mm; C_1 and C_2 are tested coefficients, $C_1 = C_2 = 1.0$.

2.3.2. Uniaxial Penetration Test

According to JTG D50-2017 [34], a cylindrical specimen with a height of 100 mm and a diameter of 150 mm was used for the uniaxial penetration test. A loading bar with a height of 50 mm and a diameter of 42 mm was used. The test temperature was set at 60 °C. The schematic diagram of this test is shown in Figure 4b. The penetration stress (σ_P), penetration strength (R_T), and penetration modulus (E_S), calculated by Equations (2)–(4), were used to assess the high-temperature deformation resistance of mixtures.

$$\sigma_P = \frac{P}{A} \quad (2)$$

$$R_T = f_T \sigma_P \quad (3)$$

$$E_S = \frac{\sigma_P}{h/H} \quad (4)$$

where P is the maximum load, N; A is the contact area, mm²; f_T is the penetration stress coefficient, with a value of 0.35; h is the penetration depth, mm; H is the height of test specimen, mm.

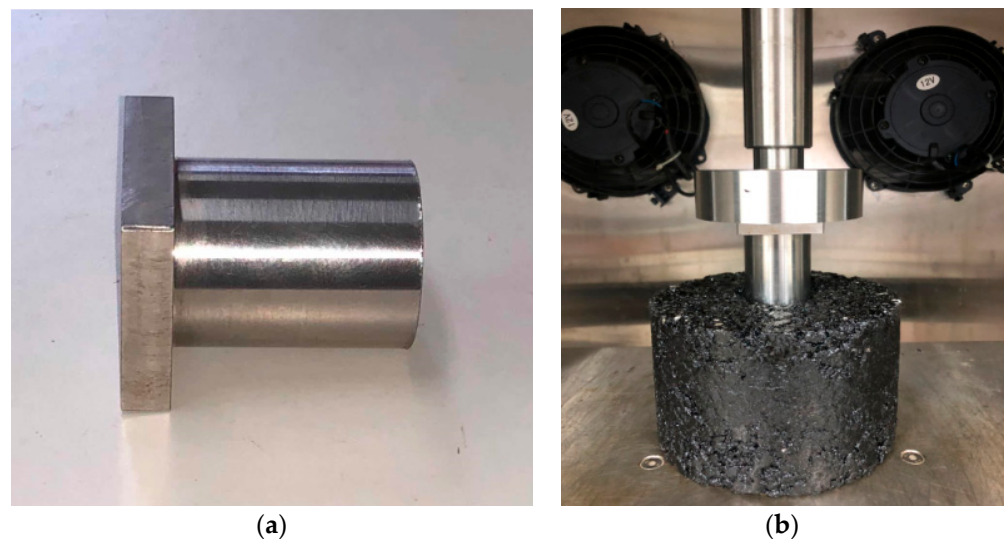


Figure 4. Schematic diagram of uniaxial penetration test: (a) Plunger; (b) Experimental set-up.

2.3.3. Dynamic Modulus Test

In order to explore the dynamic modulus of the basalt fiber-modified asphalt mixtures, five temperatures (−10 °C, 5 °C, 20 °C, 30 °C, and 50 °C) were selected for dynamic modulus test, in accordance with the Chinese specification of JTG E20- T0738 [33], along with six loading frequencies (0.1 Hz, 0.5 Hz, 1 Hz, 5 Hz, 10 Hz, and 25 Hz). The test equipment was carried out by the equipment of universal testing machine of UTM-25. The tests were conducted from low temperature to high temperature and from high frequency to low frequency. The stress control mode was adopted, and half sine load was applied to the specimen. In order to reduce the error, four duplicate test specimens in each group

were fabricated in this test. Before the test, the specimens shall be kept in an environmental chamber at the target temperature for more than 4 h. The dynamic modulus ($|E^*|$) and phase angle (ϕ) could be obtained by Equations (5) and (6), respectively.

$$|E^*| = \frac{\sigma}{\varepsilon} = \frac{\sigma_0 \sin(\omega t)}{\varepsilon_0 \sin(\omega t - \phi)} \quad (5)$$

$$\phi = \frac{t_i}{t_p} \times 360^\circ \quad (6)$$

where σ_0 (ε_0) is the maximum stress (strain); ω is the angular velocity; t_i is the lag time of the deformation peak and the load peak; t_p is the loading period.

2.3.4. Dynamic Creep Test

According to the method described in NCHRP 9-29 [35], the dynamic creep test was performed. The axial pressure was 0.7 Mpa, the contact pressure was 0.02 MPa, and the test temperature was 60 °C. In addition, half sine wave was used for repeated loading with loading time of 0.1 s and intermittent time of 0.9 s. Figure 5 presents the dynamic creep test process and the typical strain-loading time curve. The creep rate can be obtained from Stage II in Figure 5b, while another index, flow number, is the corresponding loading time of the connection point of the curves between Stage II and Stage III. In this paper, creep rate and flow number were both used to evaluate the high-temperature deformation resistance of asphalt mixtures. Generally, a smaller value of flow number and a higher value of creep rate denote that the asphalt mixtures possess worse high-temperature deformation resistance and are prone to suffering creep failure.

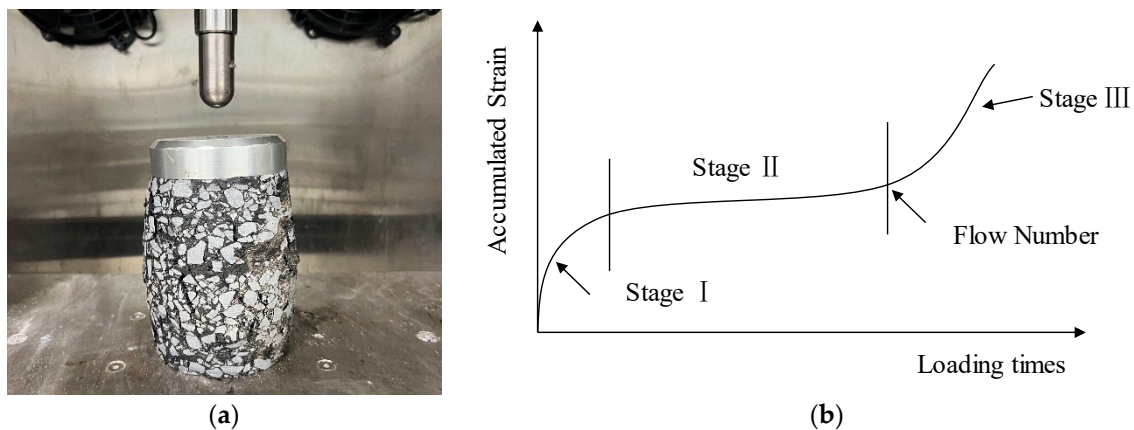


Figure 5. Dynamic creep test illustration: (a) Dynamic creep test process; (b) Illustration of three stages.

3. Results and Discussion

3.1. Results of the Wheel Tracking Test

The results of dynamic stability from the wheel tracking test are shown in Figure 6. Figure 6 revealed that the dynamic stability values of all the asphalt mixtures decreased significantly at the higher test temperature of 70 °C, no matter whether basalt fiber was added or not. For instance, the DS values of AC-13 declined sharply from 3336 times/mm to 1308 times/mm by 60.8%, while SMA-13 and SUP-13 decreased from 5673 times/mm to 3859 times/mm by 32.0%, and from 4215 times/mm to 2537 times/mm by 39.8%, respectively. Compared with the neat asphalt mixtures, the dynamic stability values of AC-13, SMA-13, and SUP-13 increased by 41.5%, 19.1%, and 25.4% at the test temperature of 60 °C, respectively, while increased by 113.0%, 40.2%, and 51.4%, respectively, at 70 °C. This phenomenon indicates that adding basalt fiber into asphalt mixtures can improve the high-temperature rutting resistance effectively, and the strengthening effect is more

significant at a higher temperature. This is due to the fact that the three-dimensional spatial distribution of basalt fiber can restrict the movement of aggregates [19]. Furthermore, in terms of the asphalt types, the DS value of AC-13 presented the highest increasing rate when adding basalt fiber. The reason may be that the original DS value of the neat sample AC-13 is small, so the percentage of improvement is relatively more obvious after the addition of basalt fiber.

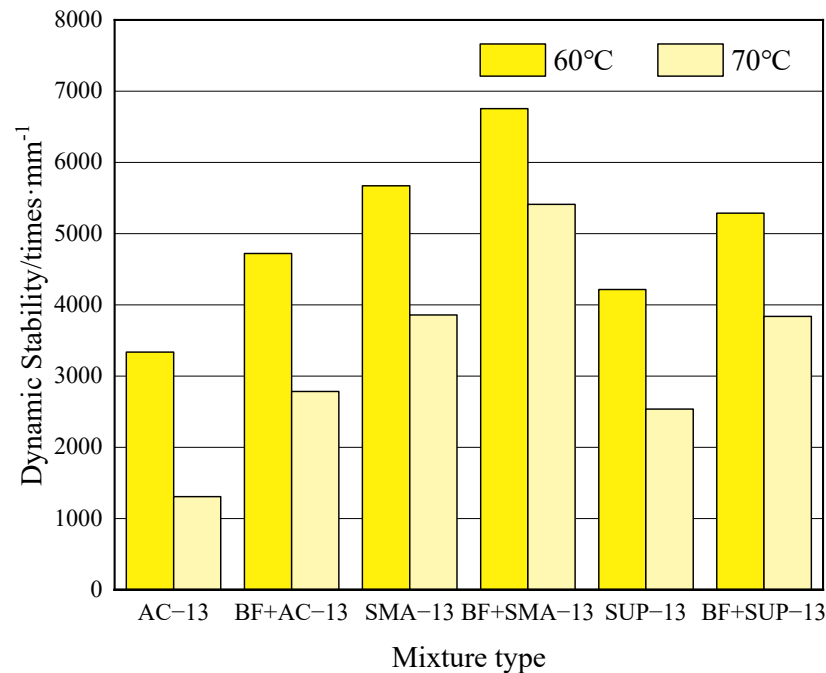


Figure 6. Results of the wheel tracking test.

3.2. Results of the Uniaxial Penetration Test

Figure 7 illustrates the results from the uniaxial penetration test. It could be found from Figure 7 that basalt fiber improved the shear stress resistance of asphalt mixtures effectively. And compared with neat asphalt mixtures, the penetration stress values of AC-13, SMA-13, and SUP-13 with basalt fiber increased from 2.63 MPa to 2.88 MPa by 9.5%, 3.48 MPa to 4.28 MPa by 23.0%, and 3.13 MPa to 3.63 MPa by 16.0%, while penetration strength values increased by 9.8%, 23.0%, and 15.5%, and penetration modulus values increased by 12.2%, 32.8%, and 26.3%, respectively. In addition, in terms of the asphalt types, it is noteworthy that SMA-13 with basalt fiber not only showed the best penetration strength but also presented the highest increasing rate. This is due to the fact that SMA gradation possesses a skeleton dense structure, and a three-dimensional network structure was formed by basalt fibers in asphalt mixtures, which controls binder drain down and improves the resistance to rutting [36].

3.3. Results of Dynamic Modulus

The master curves of dynamic modulus were constructed so as to predict the long-term mechanical properties of the asphalt mixture, which can not only represent the dynamic modulus values at various temperatures and loading frequencies but also avoid a large number of test processes. The sigmoidal model was adopted to construct dynamic modulus master curves. The fitting function was illustrated in Equation (7). Furthermore, the standard reference temperature was selected to be 20 °C.

$$\text{Log}|E^*| = \delta + \frac{\text{Max} - \delta}{1 + e^{\beta + \gamma \log f_r}} \quad (7)$$

where f_r is the load frequency at the reference temperature; δ is the minimum of the dynamic modulus, and $\delta+\alpha$ is the maximum of the dynamic modulus, namely Max; β , γ are the parameters describing the shape of the sigmoidal function.

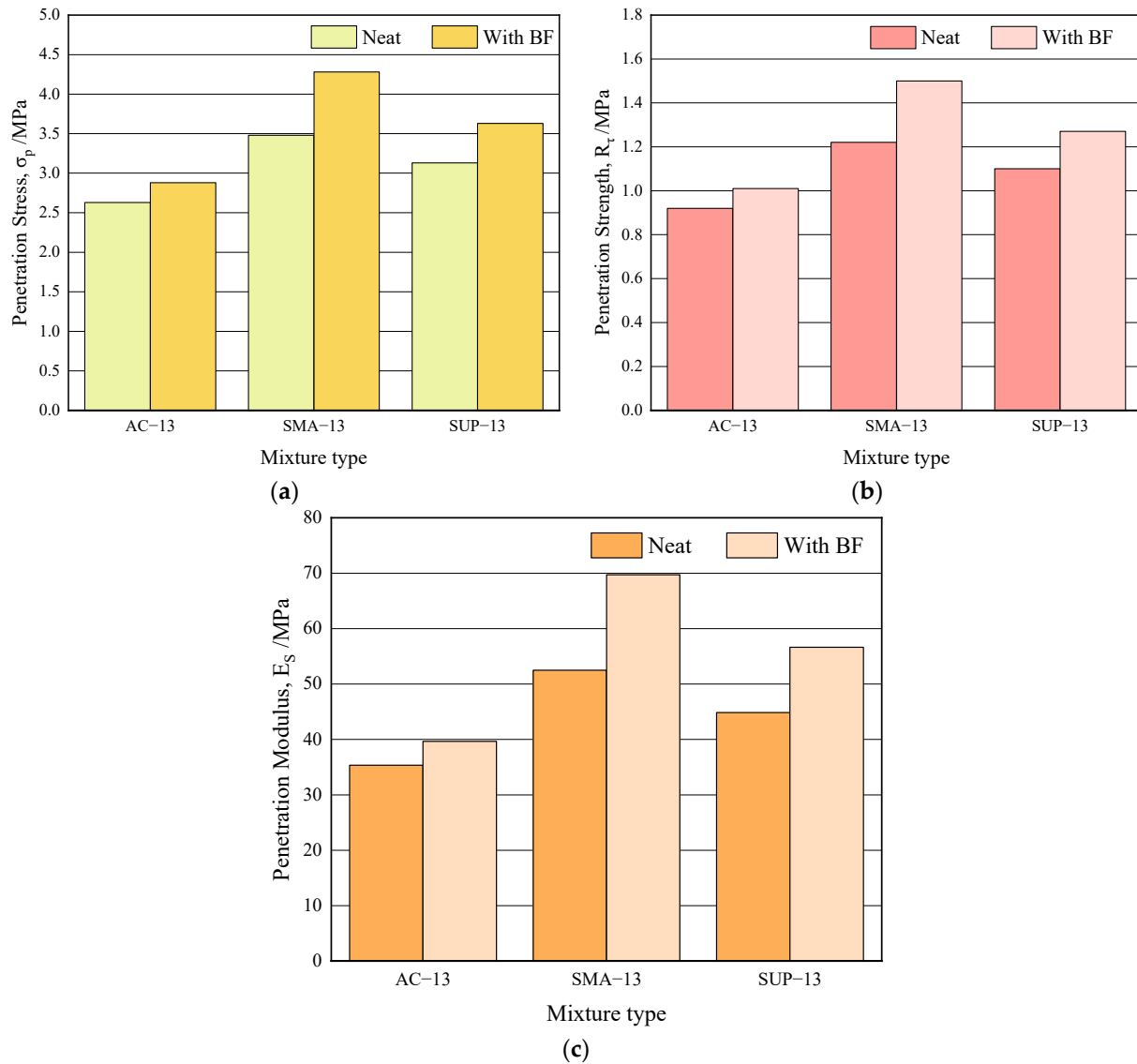


Figure 7. The results of uniaxial penetration test: (a) Penetration stress results; (b) Penetration strength results; (c) Penetration modulus results.

The dynamic modulus master curves of the six types of asphalt mixtures are illustrated in Figure 8. As seen from Figure 8, in the higher frequency section (corresponding to the low-temperature section), the dynamic modulus values of the same graded asphalt mixtures were relatively close, regardless of whether basalt fiber was added or not. However, significant differences in the dynamic modulus values could be observed in the lower frequency section (corresponding to the high-temperature section). The dynamic modulus values of asphalt mixtures with basalt fiber were much higher than that of neat asphalt mixtures without basalt fiber. Taking AC-13, for example, as shown in Figure 8a, at the reduced frequency of 10^{-3} Hz, the dynamic modulus values with basalt fiber increased from 162.44 MPa to 358.41 MPa by 120.64%, compared with neat asphalt mixtures. It indicates that the addition of basalt fiber into asphalt mixtures can reduce not only the temperature sensitivity but also enhance the elastic recovery ability, which helps increase the high-temperature stability. This result may be attributed to the formation of a basalt

fiber network in the mixtures, which plays a positive role in the reinforcement of the high-temperature deformation [37]. Moreover, another possible reason could be that the basalt fibers can absorb free asphalt and increase the number of structural asphalts [20].

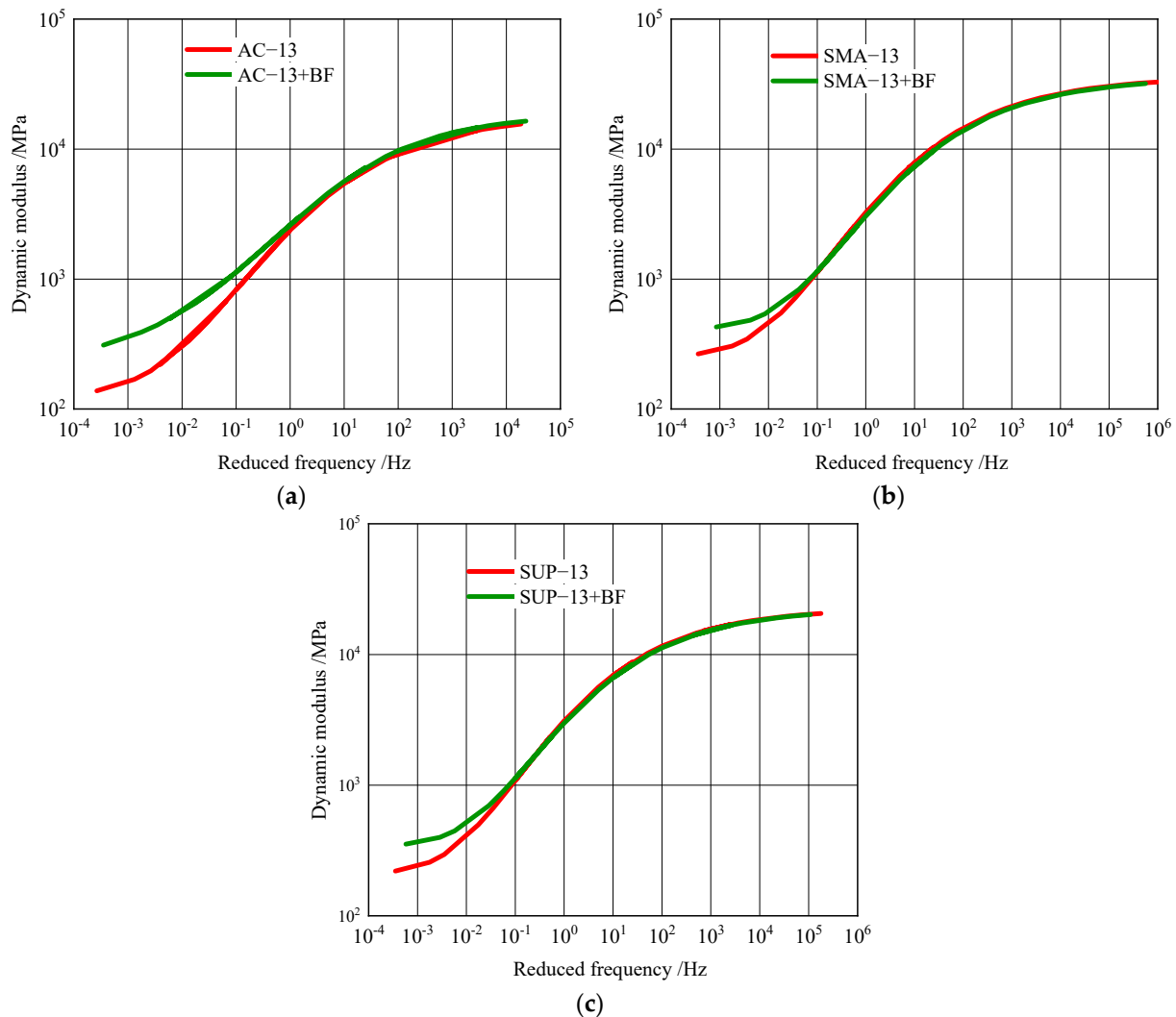


Figure 8. Dynamic modulus master curves at 20 °C: (a) Dynamic modulus master curves of AC-13; (b) Dynamic modulus master curves of SMA-13; (c) Dynamic modulus master curves of SUP-13.

In terms of mixture type, SMA-13 presented much higher dynamic modulus values than AC-13 and SUP-13 at all the test frequencies. The reason may be that the interlocking function of the coarse aggregates in SMA-13 is much more excellent than that of AC-13 and SUP-13 due to the skeleton structure, which is consistent with the findings from Chen's research [38].

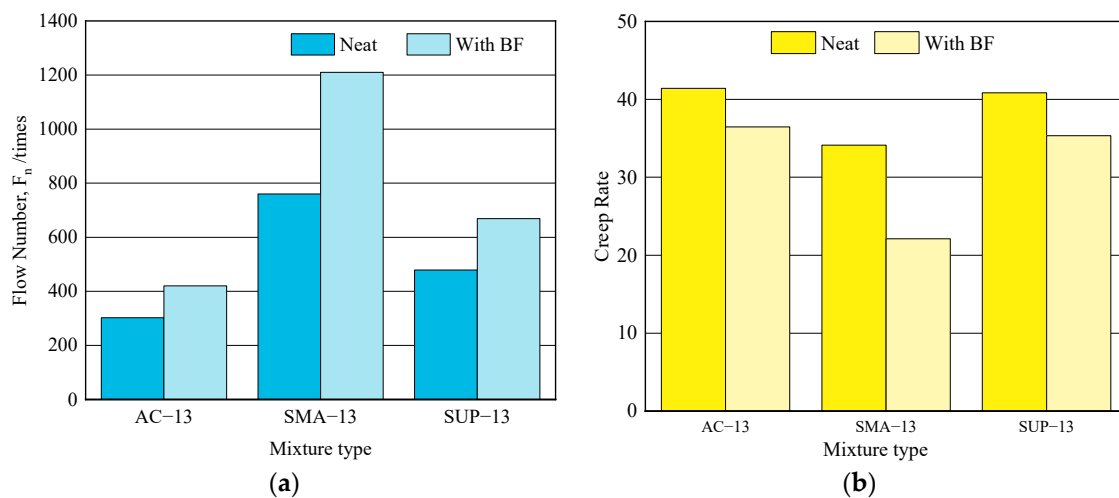
The dynamic modulus index ($|E^*|/\sin\phi$) was used to assess the anti-rutting performance, according to the recommendation in NCHRP's report [39] and Louay's study [40]. The $|E^*|/\sin\phi$ results of all the asphalt mixtures at the temperature of 50 °C and the loading frequencies of 5 Hz and 10 Hz are summarized in Table 6. It could be drawn that in terms of the same mixture type, dynamic modulus indexes $|E^*|/\sin\phi$ increased significantly when BF was added. Taking the values under 5 Hz loading frequency as examples, compared with neat asphalt mixtures, the $|E^*|/\sin\phi$ values of AC-13, SMA-13, and SUP-13 with basalt fiber increased by 9.44%, 41.53%, and 37.63%, respectively. It also could be observed that SMA-13 showed the highest $|E^*|/\sin\phi$ values, no matter adding basalt fiber or not, indicating that SMA-13 possesses better rutting resistance.

Table 6. The results of dynamic modulus indexes ($|E^*|/\sin\phi$).

Mixture Type	$ E^* /\text{MPa}(50^\circ\text{C})$		$\phi/^\circ(50^\circ\text{C})$		$ E^* /\sin\phi/\text{MPa}$	
	10 Hz	5 Hz	10 Hz	5 Hz	10 Hz	5 Hz
AC-13	535.0	389.7	34.08	31.62	954.76	743.30
BF+AC-13	622.5	441.5	34.98	32.87	1085.84	813.47
SMA-13	729.7	581.9	31.28	27.76	1405.38	1249.33
BF+SMA-13	1057.0	841.8	31.79	28.43	2006.43	1768.17
SUP-13	657.0	505.0	32.44	29.95	1224.80	1011.53
BF+SUP-13	877.0	712.0	31.54	30.76	1676.56	1392.14

3.4. Results of Dynamic Creep Test

The flow number and creep rate values from the dynamic creep test are presented in Figure 9. It could be observed that adding BF could positively enhance the dynamic creep resistance of asphalt mixtures. For instance, compared with neat asphalt mixtures, the flow number values of AC-13, SMA-13, and SUP-13 with basalt fiber increased by 39.1%, 59.2%, and 39.7%, respectively, while the creep rate values decreased by 12.0%, 35.2%, and 12.7%, respectively. It indicates that BF can efficiently delay the accumulated permanent deformation rate of asphalt mixtures. Furthermore, the enhancement effect of basalt fiber on SMA-13 was more significant than the other two types of mixtures, which is consistent with Mu's and Jomoor's [41,42] research results that SMA-13 bears a longer time to reach the Stage III of failure than AC-13 and SUP-13 due to its skeleton structure.

**Figure 9.** Results of dynamic creep test: (a) The results of flow number; (b) The results of creep rate.

3.5. Comprehensive Analysis of High-Temperature Performance Parameters

It could be noticed that adding BF can effectively improve the high-temperature rutting resistance of mixtures, which has been proved by all the parameters from the above-mentioned test methods. In order to further investigate the relationship among the different high-temperature performance parameters, dynamic stability (DS) from the wheel tracking test, penetration strength (R_T) from the uniaxial penetration test, dynamic modulus index ($|E^*|/\sin\phi$, $50^\circ\text{C}/5\text{ Hz}$) from dynamic modulus test and flow number (F_n) from dynamic creep test were selected. The correlations of dynamic stability versus penetration strength, dynamic modulus index, and flow number are plotted in Figure 10.

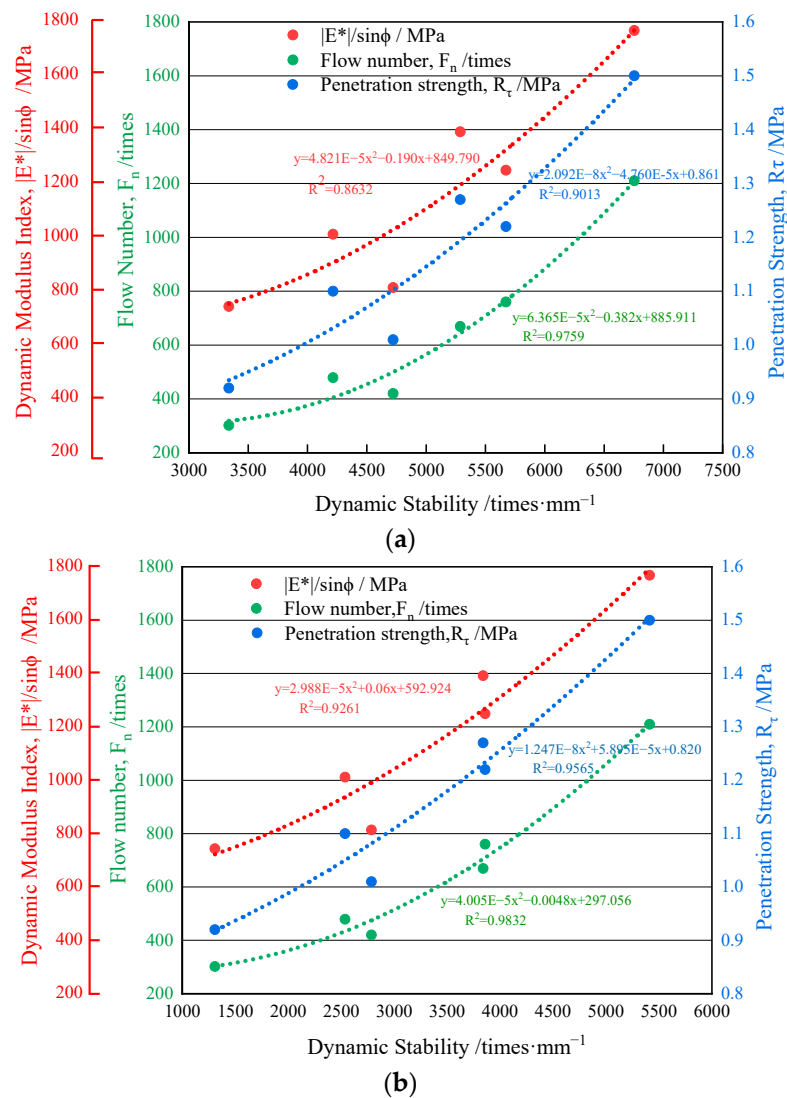


Figure 10. Correlations between DS and R_T , $|E^*|/\sin\phi$, and F_n : (a) Wheel tracking test temperature of 60 °C; (b) Wheel tracking test temperature of 70 °C.

It could be observed that approximate binomial relationships could be found between DS and the other three parameters. As shown in Figure 10a, when the wheel tracking test temperature was 60 °C, the correlation coefficients between DS and R_T , DS and $|E^*|/\sin\phi$, and DS and F_n were 0.9013, 0.8632, and 0.9759, respectively. While the correlation coefficients increased up to 0.9565, 0.9261, and 0.9832, respectively, when the temperature was 70 °C during the wheel tracking test, as illustrated in Figure 10b. It means DS values from 70 °C possess better correlations with other parameters than those from 60 °C. Moreover, it could be drawn that DS and F_n maintained good correlation coefficients over 0.97 at both test temperatures of 60 °C and 70 °C.

In brief, the approximate binomial relationships established above of different parameters can provide a certain basis for researchers to explore the high-temperature performance of asphalt mixtures with basalt fiber from different aspects. It is hoped that through this establishment, the wheel tracking test, which is a common method to test the high-temperature performance of asphalt mixture, can be used to predict the approximate values of other high-temperature performance indicators.

4. Conclusions

This paper evaluated the impact of BF on the high-temperature performance of asphalt mixtures with the gradations of AC-13, SMA-13, and SUP-13 and analyzed the correlations between different parameters; the following conclusions could be drawn in the research range:

- (1) Adding BF makes the OAC of asphalt mixtures increase by 0.1–0.2 percentage points in terms of dense graded gradations of AC-13 and SUP-13 while making the OAC decrease by 0.1–0.2 percentage points for the stone matrix asphalt of SMA-13.
- (2) Dynamic stability, penetration strength, and flow number of all types of asphalt mixtures will increase with the addition of BF, resulting in the enhancement of rutting resistance, shear stress resistance, and dynamic creep resistance of asphalt mixtures.
- (3) Adding BF can cause the asphalt mixtures to have more stiffness at high temperatures to improve the rutting resistance, presenting an increase in dynamic modulus index $|E^*|/\sin\phi$. Meanwhile, it also can make the mixtures more flexible at relatively low temperatures.
- (4) In terms of mixture type, the stone matrix asphalt SMA-13 presents superior properties to resist high-temperature deformations than AC-13 and SUP-13. Moreover, SMA-13 also shows the most significant enhancing effect by adding basalt fiber.
- (5) Approximate binomial relationships can be established between dynamic stability and penetration strength, dynamic stability and dynamic modulus index, and dynamic stability and flow number. Higher correlation coefficients can be obtained when DS values from 70 °C are used.

Author Contributions: Conceptualization, P.X., and A.K.; Data curation, A.K., and Z.W.; Formal analysis, Y.W., and Z.W.; Investigation, X.J., Y.W., and Z.W.; Methodology, X.J., P.X., and A.K.; Project administration, P.X.; Supervision, P.X.; Visualization, Y.W., and Z.W.; Writing—original draft, X.J.; Writing—review & editing, Z.W. All authors have read and agreed to the published version of the manuscript.

Funding: This research was funded by the National Natural Science Foundation of China, grant number 52178439, the Yangzhou City & University cooperation program, grant number YZ2021167, and the Yangzhou University Humanities and Social Sciences Research Fund Project, grant number xjj2020-37.

Data Availability Statement: The data presented in this study are available on request from the corresponding author.

Acknowledgments: We are grateful to all the researchers cited in the paper and the financial support of the aforementioned funds.

Conflicts of Interest: The authors declare that there are no conflict of interest in this work.

References

1. Wang, G.; Li, J.; Saberian, M.; Rahat, M.H.H.; Massarra, C.; Buckhalter, C.; Farrington, J.; Collins, T.; Johnson, J. Use of COVID-19 single-use face masks to improve the rutting resistance of asphalt pavement. *Sci. Total Environ.* **2022**, *826*, 154118. [[CrossRef](#)] [[PubMed](#)]
2. Bazzaz, M.; Darabi, M.K.; Little, D.N.; Garg, N. Effect of Evotherm-M1 on Properties of Asphaltic Materials Used at NAPMRC Testing Facility. *J. Test. Eval.* **2020**, *48*, 2256–2269. [[CrossRef](#)]
3. Liu, J.; Liu, F.Y.; Zheng, C.F.; Zhou, D.D.; Wang, L.B. Optimizing asphalt mix design through predicting the rut depth of asphalt pavement using machine learning. *Constr. Build. Mater.* **2022**, *356*, 129211. [[CrossRef](#)]
4. Guo, R.; Nian, T.F.; Zhou, F. Analysis of factors that influence anti-rutting performance of asphalt pavement. *Constr. Build. Mater.* **2020**, *254*, 119237. [[CrossRef](#)]
5. Darabi, M.K.; Huang, C.W.; Bazzaz, M.; Masad, E.A.; Little, D.N. Characterization and validation of the nonlinear viscoelastic-viscoplastic with hardening-relaxation constitutive relationship for asphalt mixtures. *Constr. Build. Mater.* **2019**, *216*, 648–660. [[CrossRef](#)]
6. Jin, D.Z.; Ge, D.D.; Zhou, X.D.; You, Z.P. Asphalt Mixture with Scrap Tire Rubber and Nylon Fiber from Waste Tires: Laboratory Performance and Preliminary M-E Design Analysis. *Buildings* **2022**, *12*, 160. [[CrossRef](#)]

7. Li, W.X.; Wang, D.Y.; Chen, B.; Hua, K.H.; Su, W.Z.; Xiong, C.L.; Zhang, X.N. Research on Three-Dimensional Morphological Characteristics Evaluation Method and Processing Quality of Coarse Aggregate. *Buildings* **2022**, *12*, 293. [[CrossRef](#)]
8. Bazzaz, M.; Darabi, M.K.; Little, D.N.; Garg, N. A Straightforward Procedure to Characterize Nonlinear Viscoelastic Response of Asphalt Concrete at High Temperatures. *Transp. Res. Rec.* **2019**, *2672*, 481–492. [[CrossRef](#)]
9. Aljubory, A.; Teama, Z.T.; Salman, H.T.; Alkareem, H.M.A. Effects of cellulose fibers on the properties of asphalt mixtures. *Mater. Today Proc.* **2021**, *42*, 2941–2947. [[CrossRef](#)]
10. Luo, D.; Khater, A.; Yue, Y.C.; Abdelsalam, M.; Zhang, Z.P.; Li, Y.Y.; Li, J.N.; Iseley, D.T. The performance of asphalt mixtures modified with lignin fiber and glass fiber: A review. *Constr. Build. Mater.* **2019**, *209*, 377–387. [[CrossRef](#)]
11. Yue, Y.C.; Abdelsalam, M.; Luo, D.; Khater, A.; Musanyufu, J.; Chen, T.B. Evaluation of the Properties of Asphalt Mixes Modified with Diatomite and Lignin Fiber: A Review. *Materials* **2019**, *12*, 400. [[CrossRef](#)] [[PubMed](#)]
12. Monaldo, E.; Nerilli, F.; Vairo, G. Basalt-based fiber-reinforced materials and structural applications in civil engineering. *Compos. Struct.* **2019**, *214*, 246–263. [[CrossRef](#)]
13. Dhand, V.; Mittal, G.; Rhee, K.Y.; Park, S.J.; Hui, D. A short review on basalt fiber reinforced polymer composites. *Compos. Part B Eng.* **2015**, *73*, 166–180. [[CrossRef](#)]
14. Guo, Q.L.; Chen, Z.P.; Liu, P.F.; Li, Y.M.; Hu, J.X.; Gao, Y.; Li, X.X. Influence of basalt fiber on mode I and II fracture properties of asphalt mixture at medium and low temperatures. *Theor. Appl. Fract. Mech.* **2021**, *112*, 102884. [[CrossRef](#)]
15. Li, Z.N.; Shen, A.Q.; Wang, H.; Guo, Y.C.; Wu, H. Effect of basalt fiber on the low-temperature performance of an asphalt mixture in a heavily frozen area. *Constr. Build. Mater.* **2020**, *253*, 119080. [[CrossRef](#)]
16. Celauro, C.; Praticò, F.G. Asphalt mixtures modified with basalt fibres for surface courses. *Constr. Build. Mater.* **2018**, *170*, 245–253. [[CrossRef](#)]
17. Guo, Q.L.; Wang, H.Y.; Gao, Y.; Jiao, Y.B.; Liu, F.C.; Dong, Z.Z. Investigation of the low-temperature properties and cracking resistance of fiber-reinforced asphalt concrete using the DIC technique. *Eng. Fract. Mech.* **2020**, *229*, 106951. [[CrossRef](#)]
18. Davar, A.; Tanzadeh, J.; Fadaee, O. Experimental evaluation of the basalt fibers and diatomite powder compound on enhanced fatigue life and tensile strength of hot mix asphalt at low temperatures. *Constr. Build. Mater.* **2017**, *153*, 238–246. [[CrossRef](#)]
19. Lou, K.K.; Kang, A.H.; Xiao, P.; Wu, Z.G.; Li, B.; Wang, X.Y. Effects of basalt fiber coated with different sizing agents on performance and microstructures of asphalt mixture. *Constr. Build. Mater.* **2021**, *266*, 121155. [[CrossRef](#)]
20. Zhang, Y.J.; Luo, W.B.; Liu, X. Experimental studies on the dynamic viscoelastic properties of basalt fiber-reinforced asphalt mixtures. *Sci. Eng. Compos. Mater.* **2021**, *28*, 489–498. [[CrossRef](#)]
21. Tan, G.J.; Wang, W.S.; Cheng, Y.C.; Wang, Y.; Zhu, Z.Q. Master Curve Establishment and Complex Modulus Evaluation of SBS-Modified Asphalt Mixture Reinforced with Basalt Fiber Based on Generalized Sigmoidal Model. *Polymers* **2020**, *12*, 1586. [[CrossRef](#)] [[PubMed](#)]
22. Guo, F.C.; Li, R.; Lu, S.H.; Bi, Y.Q.; He, H.Q. Evaluation of the Effect of Fiber Type, Length, and Content on Asphalt Properties and Asphalt Mixture Performance. *Materials* **2020**, *13*, 1556. [[CrossRef](#)] [[PubMed](#)]
23. Gao, C.M.; Han, S.; Zhu, K.X.; Wang, Z.Y. Research on Basalt Fiber Asphalt Concrete's High Temperature Performance. *Appl. Mech. Mater.* **2014**, *505–506*, 39–42. [[CrossRef](#)]
24. Fan, W.X.; Kang, H.G.; Zheng, Y.X. Experimental study of pavement performance of basalt fiber-modified asphalt mixture. *J. Southeast Univ. (Engl. Ed.)* **2010**, *26*, 614–617.
25. Fan, W.X.; Zhang, S.F.; Liu, L.Q. Laboratory Study of Marshall of Basalt Fiber-Modified Asphalt Mixture. *Appl. Mech. Mater.* **2013**, *256–259*, 1851–1857. [[CrossRef](#)]
26. Hao, M.H.; Hao, P.W. Natural Mineral Fiber Improved Asphalt Mixture Performance. *Appl. Mech. Mater.* **2014**, *638–640*, 1166–1170. [[CrossRef](#)]
27. Wang, W.S.; Cheng, Y.C.; Tan, G.J. Design Optimization of SBS-Modified Asphalt Mixture Reinforced with Eco-Friendly Basalt Fiber Based on Response Surface Methodology. *Materials* **2018**, *11*, 1311. [[CrossRef](#)] [[PubMed](#)]
28. Li, Z.X.; Guo, T.T.; Chen, Y.Z.; Zhang, M.H.; Xu, Q.Y.; Wang, J.; Jin, L.H. Study on Properties of Drainage SBS Modified Asphalt Mixture with Fiber. *Adv. Civ. Eng.* **2021**, *2021*, 7846499. [[CrossRef](#)]
29. Cheng, Y.C.; Li, L.D.; Zhou, P.L.; Zhang, Y.W.; Liu, H.B. Multi-Objective Optimization Design and Test of Compound Diatomite and Basalt Fiber Asphalt Mixture. *Materials* **2019**, *12*, 1461. [[CrossRef](#)]
30. Wu, Z.G.; Zhang, C.; Xiao, P.; Li, B.; Kang, A.H. Performance Characterization of Hot Mix Asphalt with High RAP Content and Basalt Fiber. *Materials* **2020**, *13*, 3145. [[CrossRef](#)]
31. Zhang, J.; Huang, W.; Zhang, Y.; Lv, Q.; Yan, C. Evaluating four typical fibers used for OGFC mixture modification regarding drainage, raveling, rutting and fatigue resistance. *Constr. Build. Mater.* **2020**, *253*, 119131. [[CrossRef](#)]
32. *Occupation Standard of the People's Republic of China JTG F40*; Technical Specification for Construction of Highway Asphalt Pavements; Ministry of Transport of the People's Republic of China: Beijing, China, 2004.
33. *Occupation Standard of the People's Republic of China JTG E20*; Standard Test Methods of Bitumen and Bituminous Mixtures for Highway Engineering; Ministry of Transport of the People's Republic of China: Beijing, China, 2011.
34. *Occupation Standard of the People's Republic of China JTG D50*; Specifications for Design of Highway Asphalt Pavement; Ministry of Transport of the People's Republic of China: Beijing, China, 2017.
35. National Cooperative Highway Research Program. *Simple Performance Tester for Superpave Mix Design (Project 9-29)*; Advanced Asphalt Technologies, LLC: Kearneysville, WV, USA, 2004.

36. Kumar, G.S.; Shankar, A.U.R.; Teja, B.V.S.R. Laboratory Evaluation of SMA Mixtures Made with Polymer-Modified Bitumen and Stabilizing Additives. *J. Mater. Civ. Eng.* **2019**, *31*, 4.
37. Morova, N. Investigation of usability of basalt fibers in hot mix asphalt concrete. *Constr. Build. Mater.* **2013**, *47*, 175–180. [[CrossRef](#)]
38. Chen, H.; Barbieri, D.M.; Zhang, X.M.; Hoff, I. Reliability of Calculation of Dynamic Modulus for Asphalt Mixtures Using Different Master Curve Models and Shift Factor Equations. *Materials* **2022**, *15*, 4325. [[CrossRef](#)] [[PubMed](#)]
39. National Cooperative Highway Research Program. *Simple Performance Test for Superpave Mix Design (Project 9-19 FY'98)*; NCHRP Report 465; Transportation Research Board: Washington, DC, USA, 2002.
40. Mohammad, L.N.; Wu, Z.; Obulareddy, S.; Cooper, S.; Abadie, C. Permanent Deformation Analysis of Hot-Mix Asphalt Mixtures with Simple Performance Tests and 2002 Mechanistic—Empirical Pavement Design Software. *Transp. Res. Rec.* **2006**, *1970*, 133–142. [[CrossRef](#)]
41. Mu, Y.; Fu, Z.; Liu, J.; Li, C.; Dong, W.H.; Dai, J.S. Evaluation of High-Temperature Performance of Asphalt Mixtures Based on Climatic Conditions. *Coatings* **2020**, *10*, 535. [[CrossRef](#)]
42. Jomoor, N.B.; Fakhri, M.; Keymanesh, M.R. Determining the optimum amount of recycled asphalt pavement (RAP) in warm stone matrix asphalt using dynamic creep test. *Constr. Build. Mater.* **2019**, *228*, 116736. [[CrossRef](#)]

Disclaimer/Publisher's Note: The statements, opinions and data contained in all publications are solely those of the individual author(s) and contributor(s) and not of MDPI and/or the editor(s). MDPI and/or the editor(s) disclaim responsibility for any injury to people or property resulting from any ideas, methods, instructions or products referred to in the content.